Self-organized carbon nanostrips with a new LiC_{10} structure derived from carbon nanotubes

Rachid Yazami
Division of Engineering and Applied Science, California Institute of Technology, Pasadena, California 91125 and Laboratoire d'Electrochimie et de Physicochimie des Matériaux et des Interfaces, Institut National Polytechnique de Grenoble/CNRS (UMR 5631) BP 75, 38402 St Martin d'Hères, France

Heike Gabrisch and Brent Fultz
Division of Engineering and Applied Science, California Institute of Technology, Pasadena, California 91125

(Received 23 July 2001; accepted 23 October 2001)

Single walled carbon nanotubes (SWNTs) were reacted with molten lithium at 220 °C for two weeks. This induced dramatic changes in their structure as shown by x-ray and electron diffractometry and Raman spectroscopy. A significant fraction of the initial SWNTs transformed into flat nanostrips having intercalated lithium in between them. Lithium forms a superlattice commensurate with that of the graphitelike nanostrips with $\sqrt{7}\times\sqrt{3}$ in-plane distribution. This new structure corresponds to the LiC_{10} composition. © *2001 American Institute of Physics.*
[DOI: 10.1063/1.1427704]

Although free energy is an equilibrium quantity, it has proved a useful concept for the analysis of many kinetic processes. One viewpoint of ''nonequilibrium'' materials processing considers the formation of intermediate states as the material follows different kinetic paths through a free energy surface. With this viewpoint, it follows naturally that different intermediate states can be obtained by starting at different locations on the free energy surface. Carbon single wall nanotubes (SWNTs), while interesting in their own right, are also novel starting points for the synthesis of new materials.

It seems that alkali metals form intercalation compounds with all sp^2-bonded carbon materials including fullerenes and graphite. These intercalation compounds are of basic interest. Fullerene compounds, M_xC_{60} $(1<x<3)$ where M=K, Rb, Cs, exhibit a high superconducting transition temperature (up to 40 K[1]). Interest in graphite intercalation compounds (GICs) has been further stimulated by the use of Li-intercalated graphite in anodes of commercial Li-ion batteries.[2]

In GICs, alkali metal atoms occupy the van der Waals gap between adjacent graphene layers. With increasing alkali concentration, periodic three-dimensional ordering takes place in stages, with each stage having a regular number of empty and alkali-occupied van der Waals gaps. All van der Waals gaps are occupied for stage-1 compounds. Under normal conditions, GICs with maximum metal concentration have a stage-1 structure. The compositions are LiC_6 for Li, and MC_8, for M=K, Rb and Cs. (Sodium is an exception, a stage-1 Na-GIC has not yet been synthesized.) For both metal-intercalated SWNTs and multiwalled nanotubes (MWNTs), the saturation composition is MC_8 for M=K and Rb,[3,4] which is, perhaps curiously, similar to their GIC analogues. The stoichiometry of lithium-intercalated analogues is less clear since most of these compounds have been prepared by electrochemical intercalation, where the electrolyte reactions on the carbon surface makes it difficult to determine the composition by coulometry. (The undesirable irreversible capacity associated with electrolyte decomposition is a very large 1500 mAh/g,[5] which is 40 to 50 times higher than in the best graphite materials). Lithium was reacted with MWNTs under high pressures and high temperatures.[6] At the high temperature of 400 °C, the product was mainly Li_2C_2, lithium carbide. Under high pressures a dense Li_2C compound was obtained, perhaps with Li atoms between cocentric carbon tubes.

Here we report a new material synthesized by reacting purified and annealed SWNTs[7] with molten lithium at 220 °C. SWNTs were prepared by pulsed laser ablation of graphite[8] and shaped in buckypaper of approximately 50 μm in thickness. A buckypaper sample of about 1 cm×1 cm was cut and evacuated at 200 °C for 12 h before immersion into molten lithium contained in a stainless steel reactor. The latter was then hermetically closed under high purity argon atmosphere. After two weeks, the sample was taken out of the reactor and mechanically separated from unreacted lithium on its surface. A golden color characteristic of stage-1 alkali metal GICs appeared on most parts of the sample indicating a deep lithiation. The sample was then ground gently into particles of 0.3–1 mm in size. A sample for x-ray diffraction (XRD) was prepared by inserting some powder into a capillary tube, which was then sealed under argon gas. XRD was performed using an Inel powder diffractometer equipped with a sealed Co tube and a curved detector covering 120° in 2θ angle.

Figure 1 shows the XRD patterns of SWNTs before (a) and after (b) chemical lithiation. Two broad peaks at low angle appeared in the SWNT diffractogram, together with a sharp peak at 3.37 Å corresponding to the graphitelike impurities in the sample (estimated at wt 5%). The broad peaks

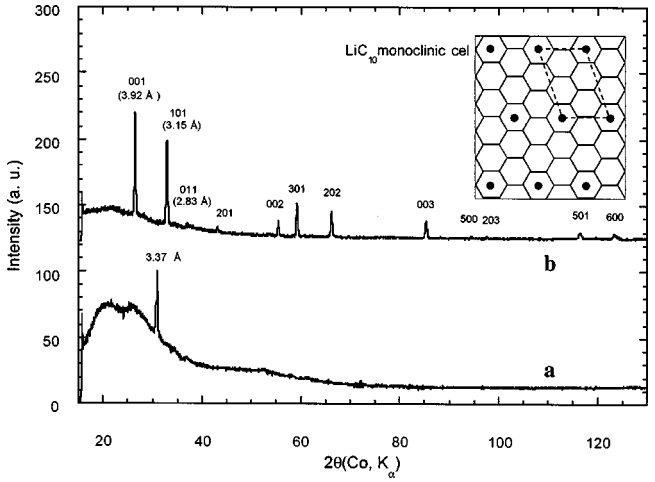

FIG. 1. X-ray diffraction patterns of SWNT material before 1(a) and after 1(b) lithiation. Note the intensity scale is logarithmic. The insert shows the $\sqrt{7}\times\sqrt{3}$ in-plane structure of LiC_{10}.

denote some disorder in the 2D triangular lattice of the SWNTs.[8] A dramatic change in the crystal structure occurs after lithiation [Fig. 1(b)]. The diffraction pattern consists of up to 12 fine lines, which were well indexed to a monoclinic cell lattice of parameters $a=6.5\,\text{Å}$, $b=4.26\,\text{Å}$, $c=3.92\,\text{Å}$, and $\gamma=109°$. This structure is consistent with a $\sqrt{7}\times\sqrt{3}$ lithium superlattice commensurate with the graphene structure as sketched in the insert. The 1D character of this new structure probably causes the differences in intensity and peak widths of the 101 and 011 diffractions.

Assuming the $\sqrt{7}\times\sqrt{3}$ in-plane structure, the composition should be LiC_{10}. To our knowledge, this is the first time that the unzipping of SWNTs is reported and the first time that LiC_{10} has been identified by XRD. The c (or $I_c=3.92\,\text{Å}$) parameter is 5 to 6% larger than for LiC_6 for which the structure is $\sqrt{3}\times\sqrt{3}$. This difference may result from the small width of carbon nanostrips (the van der Waals gap tends to be larger in nongraphitic carbons). Also, it should be noted that no lithium carbide (Li_2C_2) was detected in our sample, probably due to the lower lithiation temperature used here compared to 400 °C used by Nalimova *et al.*[6]

Raman spectra were acquired at 23 °C with the sample in a thin, Ar-filled glass structure with a Dilor XY spectrometer, working with a 514.532 nm argon excitation at low power. Figures 2(a) and 2(b) show Raman spectra of SWNTs before and after lithiation respectively. After lithiation, the low-frequency A_{1g} radial symmetry mode (also known as the ''breathing'' mode), which appears in SWNT at 186 cm^{-1} as an unresolved peak, transformed to three sharp and intense peaks at lower frequencies of 61, 75, and 114 cm^{-1} respectively (see inset). In the high frequency region, the two peaks centered at 1565 and 1592 cm^{-1} and associated mainly with the E_{2g} symmetry mode (''stretching'' mode), merged into a single unresolved peak centered at 1576 cm^{-1}. (This mode frequency is between that of highly oriented pyrolytic graphite (HOPG), 1580 cm^{-1}, and that of HOPG based LiC_6, 1569 cm^{-1}.) Raman modes in SWNTs have been discussed in detail by Rao *et al.*[9] The A_{1g} active modes, which are the signature of cylindrical graphene sheets, are still observed in the lithiated SWNTs. Not all nanotubes transformed to nanostrips (a result not determined reliably by x-ray diffractometry). The shift to lower frequencies of a sharp A_{1g} mode may indicate the formation of well-defined compositions of chemisorbed lithium along the nanotubes or within the bundles. The merging of the two high-frequency modes to a single mode at 1576 cm^{-1} is consistent with the formation of a lithium intercalated compound similar to the graphite based ones.

For transmission electron microscopy (TEM) studies, finer particles of lithiated SWNTs were deposited on an amorphous carbon membrane and transferred in a hermetic container from the dry box to the vacuum of a Philips EM420 TEM operated at 100 kV. The specimens were cooled using liquid nitrogen to minimize damage by the electron beam. Figures 3(a)–3(d) compare the SWNT material before and after lithiation. In Fig. 3(a) ropes of SWNT are shown together with their respective diffraction pattern revealing the two typical features of SWNT bundles: a row of diffractions across the forward beam and diffuse arcs oriented perpendicular to it.[10] The diffractions on the central line in Fig. 3(b) originate from the triangular arrangement of nanotubes within the bundles. Here the bundles are not aligned perfectly, causing broadening of the ''row'' of spots. The diffuse arcs can be explained by the fact that the nanotubes within the bundles exhibit a distribution in chirality.[10] Figure 3(c) shows the SWNT after lithiation. The dominant form of the material corresponds to the gray background with mottled features (see enlarged area). It seems to have lost much of the 1D texture of the SWNT bundles. Features similar to the shape of the former SWNT bundles are observed but these are in the minority and suggest the origin of the new material. A dramatic change in structure is shown by the diffraction pattern in Fig. 3(d) where the characteristics of diffraction from a SWNT bundle [Fig. 3(b)] are replaced by diffraction rings pertinent of a polycrystalline material. The *d*-spacings measured from this diffraction pattern are in

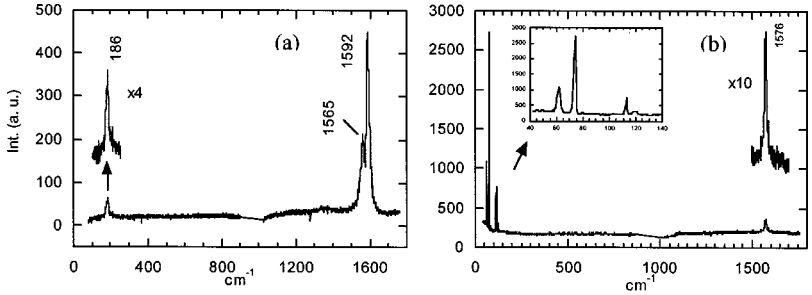

FIG. 2. Raman spectra of SWNTs before (a) and after (b) lithiation.

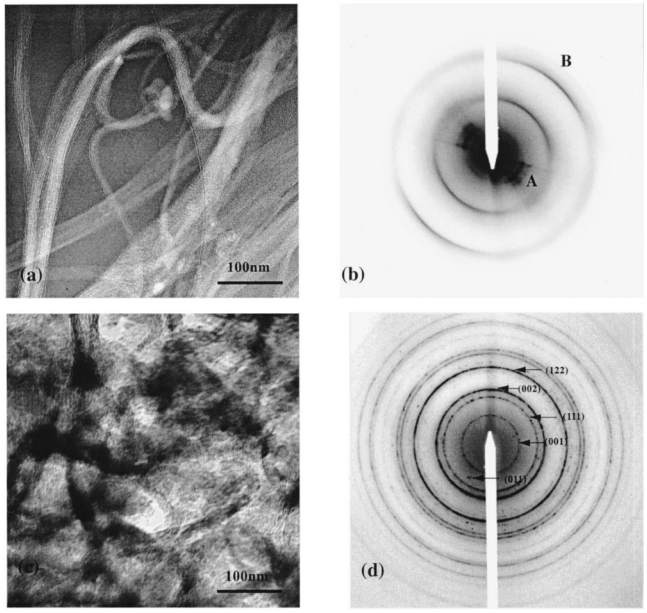

FIG. 3. Bundles of initial SWNT material (a) with characteristic diffraction pattern (b). The features in the diffraction pattern originate from the triangular arrangement of tubes within bundles (A) and a variation in chirality (B). SWNT material after lithiation (c). The majority of the LiC_6 material is evenly distributed (inset) though in some places it remains in the place of the former SWNT bundles. The diffraction pattern of the material (d) reveals a dramatic change in structure consistent with LiC_{10}.

accordance with the monoclinic structure LiC_{10} obtained by x-ray diffractometry.

Were graphite subjected to the same conditions used here to lithiate the SWNTs (220 °C, 2 weeks), diffusion-controlled kinetics would produce a series of staged compounds that nucleate and grow across the graphite crystals, culminating in a pure stage-1 LiC_6 compound.[11,12] XRD, Raman, and TEM results are consistent with the fact that upon chemical lithiation, a significant fraction of SWNTs has opened and transformed to self-organized flat graphene nanostrips, with lithium in the van der Waals gap between strips. Lithium would act as the structure stabilizer, bonding stacked nanostrips together and helping them align along the former SWNT axis direction. Therefore SWNTs undergo a transformation from tubes to flat graphene nanostrips, perhaps unzipping in the presence of lithium. Thermodynamics favors such unzipping, since the enthalpy of SWNTs is higher than that of graphite by about 10 kJ/(mole carbon atoms).[13–15] [Intercalation of lithium into graphite nanostrips is also expected to be favorable by about 8.9 kJ/(mole Li atoms)^2.] Once unzipped, the lithium epitaxial arrangement on the surface of graphene nanostrips helps them orient and stack along the new crystal axes. The similar morphologies of the bundle structures seen in Figs. 3(a) and 3(c) suggests that the initial grouping of tubes into rope structures influences the sizes and organization of the nanostrips.

Once formed, the graphite structures remain even after loss of lithium. Figure 4(a) shows graphite structures observed in a TEM sample. These structures were about 260 nm in width and a few microns in length. The diffraction pattern in Fig. 4(b) is indexed as polycrystalline graphite.

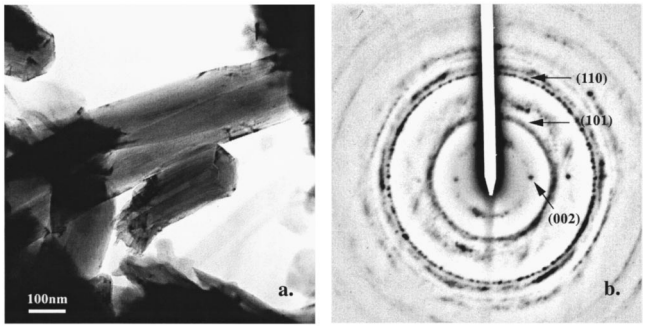

FIG. 4. TEM image (a) and diffraction pattern (b) of graphite structures in a region of material after lithiation and partial de-lithiation.

The systematic row of reflections is of ⟨002⟩ type and the *c*-direction in the image is perpendicular to the long dimension of the rods. When the sample was tilted it showed oblique texture electron diffraction pattern typical of highly-oriented graphite (HOPG). This new form of graphite may result from lithiation/delithiation process and shows a preferential alignment of graphene nanostrips along the particle axis. The prismatic shape of these highly-oriented graphitic nanostrips is unusual compared with other tubular forms of carbon such us SWNTs, MWNTs, nanofibers,[16] and fibers and filaments.[17] Further studies on the crystal structure of graphite nanostrips are currently under way.

It is interesting that the intercalated structure has the LiC_{10} composition. This structure, shown as an inset in Fig. 1, has a rectangular structure in the basal plane of the graphite. (The LiC_{10} structure can be also described with a larger base-centered orthorhombic unit cell lattice; $a=4.26$ Å, $b=13.2$ Å, and $c=3.92$ Å.) We speculate that the LiC_{10} structure is stabilized in part by the preferred orientation of a rectangular edge along the narrow width of the nanostrips, but have not identified this orientation within the plane of the sample.

ACKNOWLEDGMENTS

The authors thank Dr. C. C. Ahn for discussions and advice. This work was supported by D.O.E. through Basic Energy Sciences Grant DE-FG03-00ER15035.

[1] R. M. Fleming, A. P. Ramirez, M. J. Rosseinsky, D. W. Murphy, R. C. Raddon, S. M. Zahurak, and A. V. Makhija, Nature (London) **352**, 701 (1991).
[2] R. Yazami and P. Touzain, J. Power Sources **9**, 365 (1983).
[3] A. Thess, R. Lee, P. Nikolaev *et al.*, Science **273**, 483 (1996).
[4] O. Zhou, R. M. Fleming, D. M. Murphy, C. H. Chen, R. C. Haddon, A. P. Ramirez, and S. H. Glarum, Science **263**, 1744 (1994).
[5] B. Gao, C. Bower, J. D. Lorentzen, L. Fleming, A. Kleinhammes, X. P. Tang, L. E. McNeil, Y. Wu, and O. Zhou, Chem. Phys. Lett. **327**, 69 (2000).
[6] A. Nalimova, D. E. Slovsky, G. N. Bondarenko, H. Alvergnat-Gaucher, S. Bonnamy, and F. Beguin, Synth. Met. **88**, 89 (1997).
[7] A. G. Rinzler, J. Liu, H. Dai *et al.*, Appl. Phys. A: Mater. Sci. Process. **67**, 29 (1998).
[8] P. M. Ajayan and T. W. Ebessen, Rep. Prog. Phys. **60**, 1025 (1997).
[9] A. M. Rao, E. Richter, S. Bandow *et al.*, Science **275**, 187 (1997).
[10] L. Henrard, A. Loiseau, C. Journet, and P. Bernier, Eur. Phys. J. B **13**, 661 (2000).
[11] R. Yazami and S. Genies, Denki Kagaku **66**, 1293 (1998).

[12] J. E. Fischer, in *Chemical Physics of Intercalation*, edited by A. P. Legrand and S. Flandrois, NATO ASI Ser., Ser. B **172**, 59 (1987).
[13] P. M. Ajayan, T. Ichihashi, and S. Iijima, Chem. Phys. Lett. **202**, 384 (1993).
[14] P. M. Ajayan and S. Iijima, Nature (London) **361**, 333 (1993).
[15] G. Gao, T. Cagin, and W. A. Goddard, Nanotechnology **9**, 184 (1998).
[16] L. J. Ci, Y. H. Li, B. Q. Wei, J. Liang, C. L. Xu, and D. H. Wu, Carbon **38**, 1933 (2000).
[17] G. G. Tibbetts, G. L. Doll, D. W. Gorkiewicz, J. J. Moleski, T. A. Perry, C. J. Dasch, and M. J. Balogh, Carbon **31**, 1039 (1993).